Available online at www.sciencedirect.com
ScienceDirect
Physica A 387 (2008) 2394–2402
PHYSICA A
www.elsevier.com/locate/physa

Signal-to-noise ratio of a dynamical saturating system: Switching from stochastic resonator to signal processor

François Chapeau-Blondeau[a], Fabing Duan[b,*], Derek Abbott[c]

[a] *Laboratoire d'Ingénierie des Systèmes Automatisés (LISA), Université d'Angers, 62 avenue Notre Dame du Lac, 49000 Angers, France*
[b] *Institute of Complexity Science, Qingdao University, Qingdao 266071, PR China*
[c] *Centre for Biomedical Engineering (CBME) and School of Electrical & Electronic Engineering, The University of Adelaide, Adelaide, SA 5005, Australia*

Received 1 July 2007; received in revised form 21 August 2007
Available online 10 January 2008

Abstract

We consider an isolated dynamical saturating system for processing a noisy sinusoidal signal, and evaluate its performance with the measure of the signal-to-noise ratio. The considered system is linear for small inputs, but exhibits saturation in its response for large inputs. This nonlinearity displays the nonlinear phenomenon of stochastic resonance for a large biased sinusoid in appropriate system parameter regions. Without the stochastic resonance phenomenon, this dynamical saturating system can achieve a signal-to-noise ratio gain exceeding unity for a noisy unbiased sinusoid. These numerical results manifest the nonlinearities and the signal-processing ability of this system acting as a stochastic resonator or a signal processor.

Keywords: Dynamical saturating system; Signal-to-noise ratio gain; Stochastic resonator; Signal processor

1. Introduction

The stochastic resonance (SR) phenomenon has become one interesting research field of noise in nonlinear systems, where the action of noise improves some processing performed on a weak signal [1–5]. Initially, conventional SR has usually been defined with a quantifier such as the output signal-to-noise ratio (SNR) being a non-monotonic function of the background noise intensity, in an isolated nonlinear system driven by a subthreshold periodic input [1–5]. Then, the great majority of previous studies have focused on single element SR systems [6]. Progressively, some distinct meaningful mechanisms of SR were observed in parallel [5–12] or coupled [13–17] arrays of nonlinear systems, which significantly extend the concept of SR to broader conditions.

Briefly, these nonlinear systems exhibiting SR effects can be classified as static [5–11] and dynamic [12–17] types. Among static nonlinearities frequently used, the static threshold has been interestingly complemented by the static saturation nonlinearity [5,11]. This extended the phenomenon of SR to threshold-free nonlinearities taking the form

* Corresponding author.
E-mail addresses: chapeau@univ-angers.fr (F. Chapeau-Blondeau), fabing1974@yahoo.com.cn (F. Duan), dabbott@eleceng.adelaide.edu.au (D. Abbott).

0378-4371/$ - see front matter © 2008 Elsevier B.V. All rights reserved.
doi:10.1016/j.physa.2008.01.032

of saturating sensors [5,11]. In this novel case, SR operates with large signals, which receive assistance from the noise in order to escape from the saturating region of the response by being shifted back into the linear region of the system [5,11].

In the present paper, we study a dynamical saturating nonlinear system. Such systems, as a class of potential stochastic resonator or signal processor, are the dynamic analog of the static saturating nonlinearity of Refs. [5,11]. The system response shows linearity, when the input signal is small, but saturation for large input signal. We demonstrate the conditions where addition of noise to a large biased input sinusoid can induce the SR phenomenon. Therefore, beyond static nonlinearities with saturation [5,11], the present paper is the *first* to demonstrate the possibility of extending SR to dynamic nonlinearities with saturation.

Furthermore, we find that the SR phenomenon appears for certain pairs of system parameters. More interestingly, the SNR gain of this dynamical saturating system can be much larger than unity for an unbiased noisy sinusoidal signal in appropriate parameter conditions. Note that the SR effects disappear in this condition. These numerical results indicate that this class of saturating system is not only an alternative system exhibiting SR, but also an efficient signal processor. This dynamical saturating system deserves further studies, e.g. the SNR gain in a parallel or coupled array of such saturating systems.

This paper is organized as follows. In Section 2, the dynamic saturating system is put forward and the adequate measure of SNR is utilized to quantify the performance of this nonlinear system. In Section 3, the numerical results of the system under study are analyzed. By switching the bias of an input sinusoid on or off, this system can act as a stochastic resonator or a nonlinear signal processor. Finally, some conclusions are drawn in Section 4.

2. Dynamic saturating system and SNR

We start by considering a dynamic saturating nonlinearity defined by

$$\tau_a \frac{\mathrm{d}x(t)}{\mathrm{d}t} = -x(t) + \left[1 - \frac{x^2(t)}{X_b^2}\right][s(t) + \xi(t)], \tag{1}$$

with real parameters τ_a and X_b having units of time and amplitude, respectively [12]. Here, $s(t) = A_0 + A\sin(2\pi t/T_s)$ is a deterministic sinusoid with period T_s, bias A_0 and amplitude A. Here, $\xi(t)$ is zero-mean Gaussian white noise, independent of $s(t)$, with autocorrelation $\langle \xi(t)\xi(0)\rangle = 2D\delta(t)$ and noise intensity D. Eq. (1) exhibits saturating dynamics: When $|x(t)| \ll X_b$, then Eq. (1) reduces to linear dynamics where $\tau_a \mathrm{d}x(t)/\mathrm{d}t \approx -x(t) + s(t) + \xi(t)$, by which $x(t)$ tends to follow the noisy input $s(t) + \xi(t)$ within the lag imposed by the time constant τ_a; when $x(t)$ approaches $\pm X_b$, then the term $x(t)^2/X_b^2$ is close to one, the factor $[1 - x(t)^2/X_b^2]$ is close to zero and tends to reduce and turn off the action of the noisy input. This is the saturation effect as described in Refs. [5,11]. Strictly, when $x(t)$ reaches $\pm X_b$, the action of the noisy input is turned off, and $x(t)$ starts to relax to zero. By this mechanism, the dynamics of Eq. (1) when initialized at $x(0) \in]-X_b, X_b[$ can never exceed $\pm X_b$, and the time evolution of $x(t)$ remains confined to $[-X_b, X_b]$. Thus, the dynamics of Eq. (1) is linear at small $x(t)$ and saturates when $x(t)$ approaches $\pm X_b$. This is the dynamic analog of the static saturating nonlinearity of Ref. [5]. In this letter, we numerically integrate Eq. (1) using Euler–Maruyama discretization with a sampling time step $\Delta t \ll \tau_a$ and T_s [19,22,23]. In this realization of Gaussian white noise $\xi(t)$, we have $2D = \sigma^2 \Delta t$. Here, σ is the rms amplitude of the discrete-time implementation of $\xi(t)$ [19].

Since $s(t)$ is periodic, the system response $x(t)$ is a cyclostationary random signal. Thus, we evaluate the performance of the system by the output SNR, defined as the power contained in the output spectral line at fundamental frequency $1/T_s$ divided by the power contained in the noise background in a frequency bin ΔB around $1/T_s$, i.e.

$$R_{\mathrm{out}} = \frac{|\langle E[x(t)] \exp(-\imath 2\pi t/T_s)\rangle|^2}{\langle \mathrm{var}[x(t)]\rangle\, H(1/T_s)\Delta B}. \tag{2}$$

Here, $E[x(t)]$ is the expectation of $x(t)$ and the operator $\langle \cdots \rangle = \frac{1}{T_s}\int_0^{T_s} \cdots \mathrm{d}t$ indicates a temporal average [19]. At fixed times t and τ, the nonstationary variance of $x(t)$ is $\mathrm{var}[x(t)] = E[x^2(t)] - E^2[x(t)]$, the stationary autocovariance function of $x(t)$ is $C_{\mathrm{xx}}(\tau) = \langle \mathrm{var}[x(t)]\rangle\, h(\tau)$, and the correlation coefficient $h(\tau)$ has a Fourier

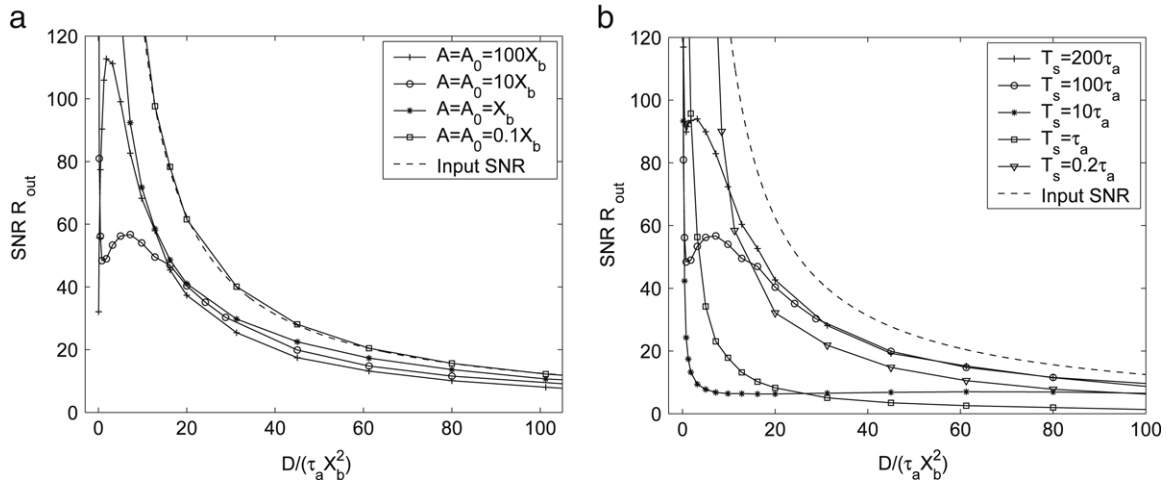

Fig. 1. Plots of SNR as a function of input noise intensity D. Output SNR R_{out} curves are marked as in the legend: (a) X_b varies, but $T_s = 100\tau_a$ and $A = A_0$; (b) τ_a changes, whereas we fix $A_0 = A = 10X_b$. Here, $s(t) = A_0 + A\sin(2\pi t/T_s)$ and the frequency bin $\Delta B = 1/T_s$. The input SNR R_{in} is also plotted in dashed lines. The sampling time $\Delta t = 10^{-3}T_s$.

transform $\mathcal{F}[h(\tau)] = H(\nu)$ [19]. In the same way, the mixture of $s(t) + \xi(t)$ has an input SNR as

$$R_{\text{in}} = \frac{A^2/4}{2D\Delta B} = \frac{A^2/4}{\sigma^2 \Delta t \Delta B} \tag{3}$$

and the SNR gain is $R_{\text{out}}/R_{\text{in}}$. The numerical method for calculating the SNR is introduced in Appendix.

3. Numerical results of stochastic resonator versus signal processor

3.1. Numerical results of stochastic resonator

Fig. 1 shows the behavior of output SNR R_{out} as a function of input noise intensity D. The SR effect appears for a biased sinusoid $s(t)$, as shown in Fig. 1. This form of SR is consistent with the result of the static saturating system considered in Refs. [5,11]. However, the SR effect disappears for a certain region of the parameter space (τ_a, X_b), as plotted in Fig. 1. The behavior of output SNR versus the noise intensity is diverse. These cases are of particular interest to be discussed.

(i) $A_0, A \ll X_b$. As stated before, the input signal $s(t)$ is quite small, i.e. , Eq. (1) reduces to linear dynamics. At $A_0 = A = 0.1X_b$ and $T_s = 100\tau_a$, as shown in Fig. 1(a), R_{out} (squares) is almost the same as R_{in} and the linearity of Eq. (1) is manifest.

(ii) Increase $A_0 = A = X_b$ and fix $T_s = 100\tau_a$, we find that R_{out} (asterisks) monotonically decreases below R_{in} when the noise power density D increases (see Fig. 1(a)). The saturating feature of Eq. (1) comes into play.

(iii) Increase further $A_0 = A \gg X_b$ and keep $T_s = 100\tau_a$. Eq. (1) is strongly nonlinear and $s(t)$ is distorted in its transmission. The SR phenomenon appears evidently as D increases, as shown in Fig. 1(a). The smaller X_b is, the more visible the resonance peak of SNR is (see R_{out} marked as circles and plus legends).

Now we keep $A_0 = A = 10X_b$ and make the system of Eq. (1) evolve in saturating dynamics. R_{out} also behaves richly when τ_a varies, as plotted in Fig. 1(b).

(iv) $T_s \ll \tau_a$. The output SNR R_{out} (down triangles) is illustrated for $T_s = 0.2\tau_a$, as shown in Fig. 1(b). The input signal $s(t)$ is much faster than the system intrinsic response time τ_a. The expectation $E[x(t)]$ is mainly restricted in the saturating regime being close to X_b for a given noise intensity, as illustrated in Fig. 2. R_{out} monotonically decreases as the noise intensity D increases.

(v) $T_s = \tau_a$. R_{out} (squares) is plotted for $T_s = \tau_a$, as shown in Fig. 1(b). The input signal $s(t)$ has the same speed as the system intrinsic response. We see that R_{out} also monotonically decreases and is lower than that of the above condition of $T_s = 0.2\tau_a$. $E[x(t)]$ has a larger amplitude and is depicted in Fig. 2.

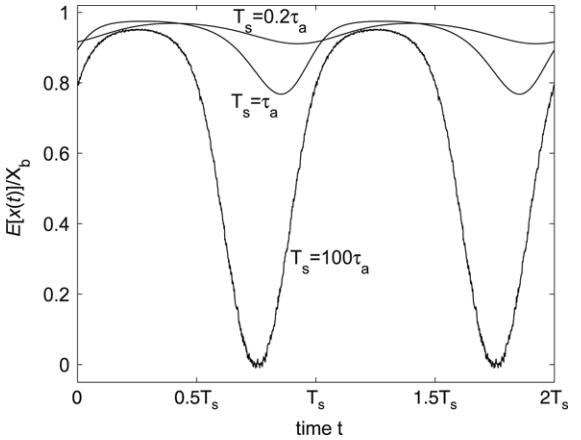

Fig. 2. Expectation $E[x(t)]$ of $x(t)$ with noise intensity $D/(\tau_a X_b^2) = 8$. Three kinds of relation between T_s and τ_a are plotted, while $A_0 = A = 10X_b$ is fixed as in Fig. 1(b).

(vi) $T_s \gg \tau_a$. The input $s(t)$ runs slow with respect to the intrinsic response time τ_a of Eq. (1). The SR effect is observed as R_{out} (circles and pluses) reaches a resonant apex and then descends slowly (see Fig. 1(b)). The expectation $E[x(t)]$ at a fixed D is also shown in Fig. 2 for comparison.

The main conclusion of discussions (i)–(vi) is that the SR phenomenon appears for strongly nonlinear regimes $A_0, A \gg X_b$ and much slower periods $T_s \gg \tau_a$. Next, we explore the corresponding probability density $\rho(x,t)$ and present some detailed descriptions of the mechanism of the SR phenomenon.

3.2. Quasi-steady state probability density $\rho(x,t)$

In the presence of noise $\xi(t)$, the statistically equivalent description for the corresponding probability density $\rho(x,t)$ is governed by the Fokker–Planck equation [22,23]

$$\tau_a \frac{\partial \rho(x,t)}{\partial t} = \left[-\frac{\partial}{\partial x} c(x) + \frac{D}{\tau_a} \frac{\partial^2}{\partial x^2} g^2(x) \right] \rho(x,t), \tag{4}$$

where $c(x,t) = -x + s(t)(1 - x^2/X_b^2)$ and $g(x) = (1 - x^2/X_b^2)$. Here, $\rho(x,t)$ obeys the natural boundary conditions such that it vanishes at $|x_b| = 1$ for any t [22]. We assume that the variation of $s(t)$ is slow enough (i.e. $T_s \gg \tau_a$) that there is enough time to make the system reach local equilibrium [1,2]. The quasi-steady state solution of Eq. (4) is given by

$$\begin{aligned} \rho(x,t) &= \frac{N}{g^2(x)} \exp\left[\frac{\tau_a}{D} \int \frac{c(x)}{g^2(x)} \mathrm{d}x \right] \\ &= N \exp\left[\frac{-\mathrm{U}(x)}{D/\tau_a} \right], \end{aligned} \tag{5}$$

where N is the normalization constant [22] and the generalized potential $U(x)$ is

$$\begin{aligned} U(x) &= \frac{D}{\tau_a} \ln[g^2(x)] - \int \frac{c(x)}{g^2(x)} \mathrm{d}x \\ &= \frac{D}{\tau_a} \ln[(1 - x^2/X_b^2)^2] + \frac{X_b^2}{2(1 - x^2/X_b^2)} - \frac{s(t) X_b}{2} [\ln(1 + x/X_b) - \ln(1 - x/X_b)]. \end{aligned} \tag{6}$$

When $s(t) = 0$, $U(x)$ has three extrema at $x = 0$ and $x = \pm\sqrt{1 - \tau_a X_b^2/(4D)}\, X_b$ as $D > \tau_a X_b^2/4$. In the presence of both $s(t)$ and $\xi(t)$, the symmetry of $U(x)$ is modulated by input signal $s(t)$ and noise density D.

Fig. 3 shows some representative curves of the generalized potential $U(x)$. Since the input signal $s(t) = A_0 + A \sin(2\pi t/T_s)$ has a varying amplitude ranging from zero to $2A$ ($A_0 = A$), the right well of generalized potential

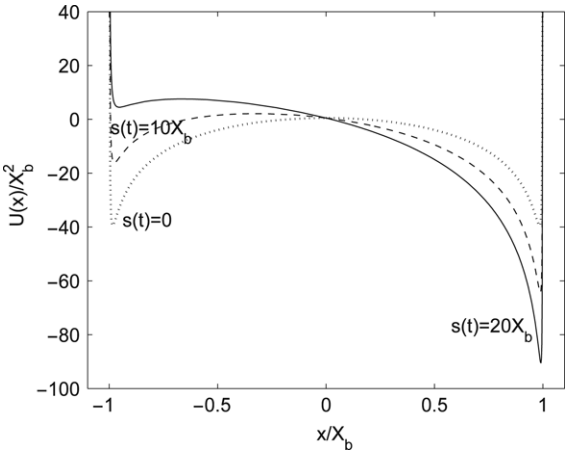

Fig. 3. The generalized potential $U(x)$ at $D/(\tau_a X_b^2) = 8$. There representative values of $s(t) = A_0 + A\sin(2\pi t/T_s)$ are plotted for $A = A_0 = 10X_b$ and $T_s = 100\tau_a$.

$U(x)$ is rising. The modality of $\rho(x,t)$ is determined by the number of minima of $U(x)$. Therefore, $\rho(x,t)$ will be bimodal as the cubic $U'(x) = 0$ has three real roots given as the discriminant relation

$$\frac{q^2}{4} + \frac{p^3}{27} > 0,$$
$$q = \frac{4s^3(t)}{27}\left(\frac{\tau_a X_b^2}{4D}\right)^3 - \frac{s(t)\tau_a X_b^4}{12D}\left(\frac{\tau_a X_b^2}{4D} - 4\right),$$
$$p = X_b^2\left(\frac{\tau_a X_b^2}{4D} - 1\right) - \frac{s^2(t)}{3}\left(\frac{\tau_a X_b^2}{4D}\right)^2. \tag{7}$$

This feature of the generalized potential $U(x)$ is pertinent to that of the bistable potential discussed in Refs. [12–15,17]. Note that the generalized potential $U(x)$ of Eq. (6) is dependent on not only signal amplitude and system parameters, but also the noise intensity, which is a random potential in this sense [22]. The appearance of SR effects is also closely associated with the bimodal $\rho(x,t)$. Note that the generalized potential $U(x)$ and the quasi-steady state probability density function $\rho(x,t)$ have similar behaviors in the Stratonovich sense (not shown here) [1,31–33].

The conventional SR theory of Ref. [2] has been applied in the multiplicative noise condition [1,31–33]. This paper mainly focuses on the numerical result of this dynamical saturating system. The generalized potential and the quasi-steady state probability density express certain aspects of SR effects. Next, the statistical characteristics will be numerically presented and help us to understand the SR mechanism in detail.

3.3. Expectation $E[x(t)]$ and stationary autocovariance function $C_{xx}(\tau)$

We select three values of $D/(\tau_a X_b^2) = 1.25$, 8 and 20 at the SR-type curve (circles) of input sinusoidal signal with frequency $T_s = 100\tau_a$, amplitude $A = 10X_b$ and bias $A_0 = A$, as plotted in Fig. 1. The corresponding mean functions $E[x(t)]$ and the stationary autocovariance functions $C_{xx}(\tau)$ are plotted in Fig. 4(a) and (b), respectively. It is seen that the periodic function $E[x(t)]$ has a period of T_s and a decreasing amplitude as D increases, whereas the stationary autocovariance function $C_{xx}(\tau)$ varies richly. Generally, the output noise is a Lorentz-like colored noise with the correlation time τ_r. Here, τ_r can be calculated by $h(|\tau| \geq \tau_r)$ less than a small value ε. The nonstationary variance $\langle \mathrm{var}[x(t)]\rangle = C_{xx}(0)$ defined in Eq. (2) increases as noise intensity D increases, while the correlation time τ_r decreases. The nonlinear variations of $E[x(t)]$ and $C_{xx}(\tau)$ result in the phenomenon of SR, as discussed in Ref. [12].

3.4. Numerical results of nonlinear signal processor

The literature points out that SR does not provide a mechanism by which the output SNR of a weak input sinusoidal signal can be enhanced beyond the input SNR in a Gaussian noise background [24–26], as this would require the

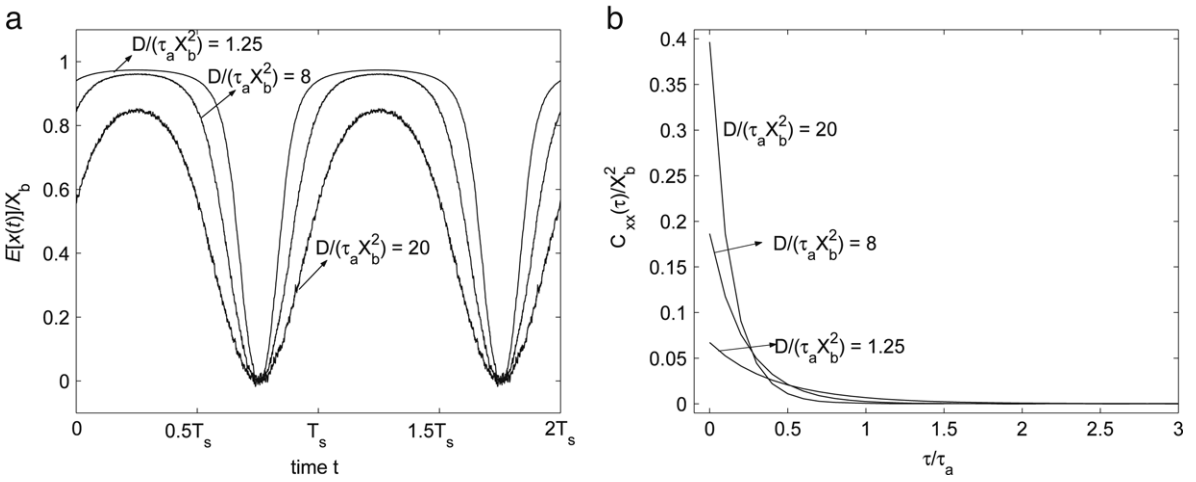

Fig. 4. Temporal behaviors of (a) $E[x(t)]$ and (b) $C_{\mathrm{xx}}(\tau)$ for input sinusoidal signal $s(t) = A_0 + A\sin(2\pi t/T_s)$ with frequency $T_s = 100\tau_a$ and amplitude $A = A_0 = 10X_b$ at three different values of $D/(\tau_a X_b^2) = 1.25$, 8 and 20. Other parameters are the same as in Fig. 1.

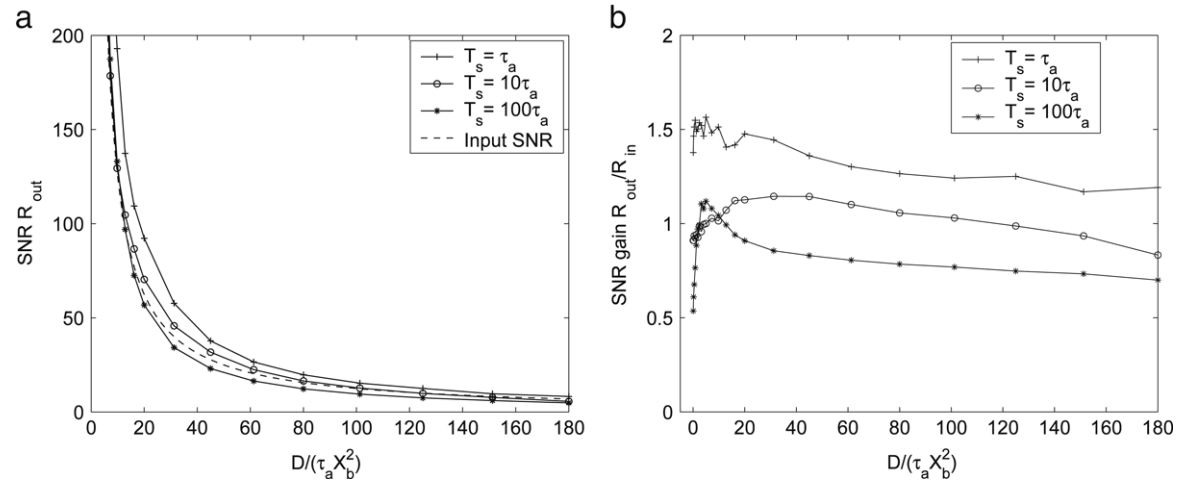

Fig. 5. Plots of (a) the SNR R_{out} and (b) the SNR gain $R_{\mathrm{out}}/R_{\mathrm{in}}$ versus the noise intensity D. Here, $A = 10X_b$ and $A_0 = 0$ and $T_s = 100\tau_a$. The signal period T_s is inserted in the legends. The input SNR R_{in} is also plotted in dashed lines.

SNR gain to exceed unity. This statement is based on linear response theory. However, beyond the regime where linear response theory applies, it has been demonstrated that the SNR gain can indeed exceed unity in non-dynamical systems, [5,10,11,18] and dynamical systems, [20,21,27–30]. The corresponding input SNR R_{in} (dashed lines) is also depicted in Fig. 1. In comparison with the output SNR R_{out}, Fig. 1 tells that the output SNR of a noisy signal caused by its transduction through a nonlinear system seems to be low. In this paper, the discussed signal amplitude is not too weak to the noise intensity and $A = 10X_b$ is frequently employed in illustrative examples of Figs. 1–4. Naturally, we should find in which condition the output SNR can exceed the input SNR, and how high the SNR gain can reach for a given noise intensity.

Fig. 5 shows the output SNR R_{out} and the SNR gain $R_{\mathrm{out}}/R_{\mathrm{in}}$ as a function of the noise intensity D. The input signal $s(t) = A\sin(2\pi t/T_s)$ with $A_0 = 0$, $A = 10X_b$ and $T_s = 100\tau_a$. When the system parameters (τ_a, X_b) vary, the SNR gain can exceed unity and is up to 1.55 at low noise intensity, as plotted in Fig. 5(b). It is emphasized that no SR effects occur for the input unbiased $s(t) = A\sin(2\pi t/T_s)$ (other results not shown). We are more interesting in the behavior of SNR gain at a given moderate noise intensity. Here, we select a moderate noise intensity $D/(\tau_a X_b^2) = 80$ and the input SNR $R_{\mathrm{in}} = 15.625$. Tune the pair of parameters (τ_a, X_b) and plot the contour of SNR gain in Fig. 6. In the regimes of $0.3 \leq \tau_a/T_s \leq 0.8$ and $0.05 \leq X_b/A \leq 2.5$, the SNR gain is larger than 1.3641. This indicates the

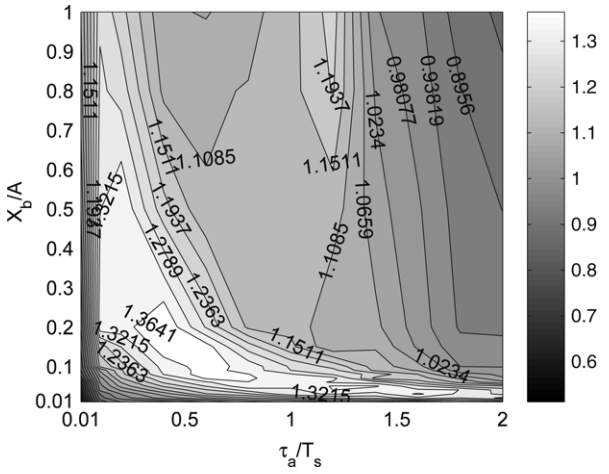

Fig. 6. Contour plot of SNR gain versus system parameters (τ_a, X_b). The noise intensity is chosen at the point of $D/(\tau_a X_b^2) = 80$ in Fig. 5 and the corresponding input SNR $R_{\text{in}} = 15.625$. Other parameters are the same as in Fig. 5.

robustness of the dynamical saturating system of Eq. (1), i.e. many tunable pairs of parameters (τ_a, X_b) eliciting higher SNR gain. In this parameter region, one highest SNR gain reaches 1.4 at $\tau_a/T_s = 0.6$ and $X_b/A = 0.1$. Combining with the more higher SNR gain of 1.55 in Fig. 5, these results are better than that obtained in an isolated bistable system with an input noisy sinusoidal signal [27,12]. The maximal SNR gain around 1.2 is obtained in Ref. [27]. Therefore, this point represents the powerful signal-processing ability of the dynamical saturating system of Eq. (1). In brief, when we turn off the bias A_0, the dynamical saturating system can switch from a stochastic resonator to a signal processor capable of amplifying the SNR.

4. Conclusion

In this paper, we propose a dynamical saturating system and numerically study its nonlinearity in terms of the output SNR and SNR gain. Some numerical characteristics of the dynamical saturating system are detailedly observed. The output SNR shows a resonant-like behavior for a noisy sinusoidal signal with large bias as the noise intensity increases; this is the phenomenon of SR. However, this SR effect disappears for certain parameters. In the condition of a noisy unbiased input, we study the signal-processing ability of this saturating system without SR phenomena. The SNR gain can exceed unity for certain system parameters. When we fixed the input SNR and tuned system parameters, the SNR gain shows that quite a large parameter region is beyond unity. It indicates the robustness of this dynamical saturating system for obtaining high SNR gain in the parameter space. This interesting saturating system of Eq. (1), with the structure of parallel or coupled array, deserves to be further studied in other signal processing problems.

Acknowledgments

We gratefully thank the anonymous reviewers for their constructive comments and suggestions. This work is sponsored by NSFC (No. 60602040), Taishan Scholar CPSP, the SRF for ROCS, SEM and PhD PFME of China (No. 20051065002). Funding from the Australian Research Council (ARC) is gratefully acknowledged.

Appendix. Numerical method for computing the power spectrum

The corresponding measured power spectrum of the cyclostationary response $x(t)$ is computed in the following way that is based on the theoretical derivations contained in Refs. [5,19]. The definition of Eq. (2) involves ensemble averages $E[\cdot]$ and temporal averages denoted by $\langle \cdots \rangle$, which can be computed from a single temporal realization of the signal.

The total evolution time of Eq. (1) is $(K + 1)T_s$, while the first period of data is discarded to skip the start-up transient [27]. In each period T_s, the time scale is discretized with a sampling time $\Delta t \ll T_s$ such that $T_s = L\Delta t$. The

white noise is with a correlation duration much smaller than T_s and Δt. We choose a frequency bin $\Delta B = 1/T_s$, and we shall stick to $\Delta t \Delta B = 10^{-3}$, $L = 1000$ and $K \geq 10^5$ in this paper [12,19]. In succession, we follow:

(**a**) The estimation of the mean $E[x(j\Delta t)]$ is obtained over one period $[0, T_s[$, and the precise time $j\Delta t$ of $E[x(j\Delta t)]$ ($j = 0, 1, \ldots, L-1$) shall be tracked correctly in each periodic evolution of Eq. (4), i.e. $[kT_s, (k+1)T_s[$ for $k = 1, 2, \ldots, K$.

(**b**) For a fixed time of $\tau = i\Delta t$, the products $y(j\Delta t)x(j\Delta t + i\Delta t)$ are calculated for $j = 1, 2, \ldots, KT_s/\Delta t$. Here, $i = 0, 1, \ldots, \tau_{\max}/\Delta t$. The estimation of the expectation $E[x(j\Delta t)x(j\Delta t + i\Delta t)]$ and $E[x(j\Delta t)]E[x(j\Delta t + i\Delta t)]$ are then performed over a time domain $\tau \in [0, \tau_{\max}[$. Immediately, the stationary autocovariance function $C_{xx}(i\Delta t)$ can be computed [12,19]. Note the time $\tau_{\max}$ is selected in such a way that at $\tau_{\max}$, the stationary autocovariance function $C_{xx}(i\Delta t)$ has returned to zero. In practice, we can select a quite small positive real number ε. If $C_{xx}(i\Delta t)/C_{xx}(0) \leq \varepsilon$, the above computation shall be ceased and the index i_{end} is found, leading to $\tau_{\max} = i_{\text{end}}\Delta t$.

(**c**) Upon increasing the total evolution time of Eq. (1) as $(K'+1)T_s$ ($K' > K$), and evaluate the mean $E'[x(j\Delta t)]$ and the stationary autocovariance function $C'_{xx}(i\Delta t)$ again. If the differences between $E'[x(j\Delta t)]$ and $E[x(j\Delta t)]$, $C'_{xx}[i\Delta t]$ and $C_{xx}(i\Delta t)$, converged within an allowable tolerance, we go to the next step (**d**). If they do not converge, the total evolution time of Eq. (1) should be increased to $(K''+1)T_s$ larger than $(K'+1)T_s$, until the convergence is realized.

(**d**) With the converged mean $E[x(j\Delta t)]$ and stationary autocovariance function $C_{xx}(i\Delta t)$, the corresponding SNR of Eq. (2) in the noise background around $1/T_s$ can be numerically developed.

References

[1] L. Gammaitoni, P. Hänggi, P. Jung, F. Marchesoni, Stochastic resonance, Rev. Modern Phys. 70 (1998) 233–287.
[2] B. McNamara, K. Wiensenfeld, Theory of stochastic resonance, Phys. Rev. A 39 (1989) 4854–4869.
[3] G. Schmid, P. Hänggi, Controlling nonlinear stochastic resonance by harmonic mixing, Physica A 351 (2005) 95–105.
[4] G.P. Harmer, D. Abbott, Motion detection and stochastic resonance in noisy environments, Microelectronics J. 32 (2001) 959–967.
[5] F. Chapeau-Blondeau, D. Rousseau, Noise-aided SNR amplification by parallel arrays of sensors with saturation, Phys. Lett. A 351 (2006) 231–237.
[6] N.G. Stocks, Information transmission in parallel threshold arrays: Suprathreshold stochastic resonance, Phys. Rev. E 63 (2001) 041114.
[7] M.D. McDonnell, D. Abbott, C.E.M. Pearce, An analysis of noise enhanced information transmission in an array of comparators, Microelectronics J. 33 (2002) 10791089.
[8] N.G. Stocks, Suprathreshold stochastic resonance in multilevel threshold systems, Phys. Rev. Lett. 84 (2000) 2310–2313.
[9] P. Jung, G. Mayer-Kress, Spatiotemporal stochastic resonance in excitable media, Phys. Rev. Lett. 74 (1995) 2130–2133.
[10] F. Chapeau-Blondeau, D. Rousseau, Enhancement by noise in parallel arrays of sensors with power-law characteristics, Phys. Rev. E 70 (2004) 060101(R).
[11] D. Rousseau, J. Rojas Varela, F. Chapeau-Blondeau, Stochastic resonance for nonlinear sensors with saturation, Phys. Rev. E 67 (2003) 021102.
[12] F. Duan, F. Chapeau-Blondeau, D. Abbott, Noise improvement of SNR gain in parallel array of bistable dynamic systems by array stochastic resonance, Electron. Lett. 42 (2006) 1008–1009.
[13] M.E. Inchiosa, A.R. Bulsara, Signal detection statistics of stochastic resonators, Phys. Rev. E 53 (1996) R2021–R2024.
[14] M.E. Inchiosa, A.R. Bulsara, Nonlinear dynamic elements with noisy sinusoidal forcing: Enhancing response via nonlinear coupling, Phys. Rev. E 52 (1995) 327–339.
[15] J.F. Lindner, B.K. Meadows, W.L. Ditto, M.E. Inchiosa, A.R. Bulsara, Array enhanced stochastic resonance and spatiotemporal synchronization, Phys. Rev. Lett. 75 (1995) 3–6.
[16] L. Fortuna, M. Frasca, M. La Rosa, A. Spata, Dynamics of neuron populations in noisy environments, Chaos 15 (2005) 014102.
[17] J.M. Casado, J. Gómez-Ordóñez, M. Morillo, Stochastic resonance of collective variables in finite sets of interacting identical subsystems, Phys. Rev. E 73 (2006) 011109.
[18] K. Loerincz, Z. Gingl, L.B. Kiss, A stochastic resonator is able to greatly improve signal-to-noise ratio, Phys. Lett. A 224 (1996) 63–67.
[19] F. Chapeau-Blondeau, X. Godivier, Theory of stochastic resonance in signal transmission by static nonlinear systems, Phys. Rev. E 55 (1997) 1478–1495.
[20] Z. Gingl, R. Vajtai, L.B. Kiss, Signal-to-noise gain by stochastic resonance in a bistable system, Chaos Solitons Fractals 11 (2000) 1929–1932.
[21] J. Casado-Pascual, J. Gómez-Ordóñez, M. Morillo, Phys. Rev. Lett. 91 (2003) 210601.
[22] H. Risken, The Fokker–Planck Equation, 2nd ed., in: Springer Series in Synergetics, vol. 18, Springer-Verlag, Berlin, 1989.
[23] C.W. Gardiner, Handbook of Stochastic Methods, 2nd ed., in: Springer Series in Synergetics, vol. 13, Springer-Verlag, Berlin, 1989.
[24] M.I. Dykman, P.V.E. McClintock, What can stochastic resonance do? Nature 391 (1998) 344.
[25] M.I. Dykman, R. Mannella, P.V.E. McClintock, N.G. Stocks, Fluctuation-induced transitions between periodic attractors: Observation of supernarrow spectral peaks near a kinetic phase transition, Phys. Rev. E 65 (1995) 48–51.
[26] A. Neiman, L. Schimansky-Geier, F. Moss, Linear response theory applied to stochastic resonance in models of ensembles of oscillators, Phys. Rev. E 56 (1997) R9–R12.

[27] P. Hänggi, M.E. Inchiosa, D. Fogliatti, A.R. Bulsara, Nonlinear stochastic resonance: The saga of anomalous output–input gain, Phys. Rev. E 62 (2000) 6155–6163.
[28] V.N. Chizhevsky, G. Giacomelli, Improvement of signal-to-noise ratio in a bistable optical system: Comparison between vibrational and stochastic resonance, Phys. Rev. A 71 (2005) 011801.
[29] M.E. Inchiosa, A.R. Bulsara, A.D. Hibbs, B.R. Whitecotton, Signal enhancement in a nonlinear transfer characteristic, Phys. Rev. Lett. 80 (1998) 1381–1384.
[30] M.A. Fuentes, R. Toral, H.S. Wio, Enhancement of stochastic resonance: The role of non Gaussian noises, Physica A 295 (2001) 114–122.
[31] L. Gammaitoni, F. Marchesoni, E. Menichella-Saetta, S. Santucci, Multiplicative stochastic resonance, Phys. Rev. E 49 (1994) 4878–4881.
[32] Y. Jia, S. Yu, J. Li, Stochastic resonance in a bistable system subject to multiplicative and additive noise, Phys. Rev. E 62 (2000) 1869–1878.
[33] B. Xu, J. Li, J. Zheng, Parameter-induced aperiodic stochastic resonance in the presence of multiplicative noise and additive noise, Physica A 343 (2004) 156–166.